Published in final edited form as:
Hepatology. 2010 October ; 52(4): 1390–1400. doi:10.1002/hep.23795.

CX3CL1-CX3CR1 interaction prevents CCl_4-induced liver inflammation and fibrosis

Tomonori Aoyama, **Sayaka Inokuchi**, **David A. Brenner**, and **Ekihiro Seki**
Division of Gastroenterology, Department of Medicine, University of California San Diego, School of Medicine. La Jolla, CA, 92093

Tomonori Aoyama: taoyama@ucsd.edu; Sayaka Inokuchi: sinokuchi@ucsd.edu; David A. Brenner: dbrenner@ucsd.edu; Ekihiro Seki: ekseki@ucsd.edu

Abstract

Chronic liver disease is associated with hepatocyte injury, inflammation and fibrosis, in which chemokines and chemokine receptors are key factors for the migration of inflammatory cells including macrophages and non-inflammatory cells such as hepatic stellate cells (HSCs). The expression of CX3CR1 and its ligand CX3CL1 (Fractalkine) is upregulated in chronic liver diseases, such as chronic hepatitis C. However, the precise role of CX3CR1 in the liver is still unclear. Here we investigated the role of the CX3CL1-CX3CR1 interaction in a carbon tetrachloride (CCl_4)-induced liver inflammation and fibrosis model. CX3CR1 is dominantly expressed on Kupffer cells in the liver. In contrast, the main source of CX3CL1 is HSC. Mice deficient in CX3CR1 showed a significant increase of inflammatory cell recruitment and cytokine production, including TNF-α, MCP-1, MIP-1β and RANTES after CCl_4 treatment compared to WT mice, suggesting that CX3CR1 signaling prevents liver inflammation. Kupffer cells in CX3CR1-deficient mice after CCl_4 treatment had increased expression of TNF-α and TGF-β, and reduced expression of the anti-inflammatory markers IL-10 and arginase-1. Co-culture experiments showed that HSCs had significantly greater activation by Kupffer cells from CCl_4-treated CX3CR1-deficient mice compared to those from WT mice. Indeed, augmented fibrosis was observed in CX3CR1-deficient mice compared to WT mice after CCl_4 treatment. Finally, CX3CL1 treatment induced the expression of IL-10 and arginase-1 in WT cultured Kupffer cells through CX3CR1, which in turn suppress HSC activation. In conclusion, CX3CL1-CX3CR1 interaction inhibits inflammatory properties in Kupffer cells/macrophages resulting in decreased liver inflammation and fibrosis.

Keywords

chemokine; chemokine receptor; hepatic stellate cell; Kupffer cell

Introduction

Liver inflammation is caused by hepatocyte damage that is associated with acute and chronic liver diseases including alcoholic liver diseases, hepatitis B and C, and non-alcoholic steatohepatitis. In liver inflammation, various types of cells including natural killer cells, natural killer T cells, T cells, dendritic cells and macrophages, are recruited and

Correspondence: Ekihiro Seki; Division of Gastroenterology, Department of Medicine, University of California, San Diego, School of Medicine, 9500 Gilman Drive MC#0702, Leichatag Biomedical Research Building Rm#332MM, La Jolla, CA, 92093-0702; ekseki@ucsd.edu; Tel. (858) 822-5339, Fax. (858) 822-5370.

No conflicts of interest exist.

activated(1,2). In particular, the hepatic resident macrophage, the Kupffer cell, is a key player to produce inflammatory cytokines and reactive oxygen species to provoke liver inflammation upon liver injury(1). Both inflammatory cytokines including TNF-α, IL-1β and IL-6 and anti-inflammatory cytokines including IL-10 are produced by Kupffer cells(1). It is suggested that the balance between pro-inflammatory and anti-inflammatory responses is strictly regulated. Sustained and chronic liver injury and inflammation activate hepatic stellate cells (HSCs) and cause liver fibrosis. Following liver injury, activated Kupffer cells produce various inflammatory and fibrogenic cytokines, such as MCP-1 and TGF-β that lead to trans-differentiation of quiescent HSCs to myofibroblasts. Myofibroblasts express α-smooth muscle actin (SMA) and produce extra cellular matrix (ECM) proteins, such as collagen type I, III and IV in the liver(3,4). The excessive production and deposition of ECM proteins result in liver fibrosis. Kupffer cell-derived TGF-β is essential for HSC activation, and Kupffer cell-depleted animals showed a significant reduction of liver fibrosis, indicating that Kupffer cells are required for HSC activation and fibrogenic responses(5). Thus, the interaction of Kupffer cells with HSCs is crucial for HSC activation in chronic liver disease.

Chemokines are small, secreted proteins that promote cell migration, chemotaxis and cell homing, which is a key event in the development under normal conditions and of inflammation and disease in pathological conditions including neovascularization, fibrosis, cancer cell growth and metastasis(6,7). Chemokines are classified into four subfamilies C, CC, CXC and CX3C chemokines. Chemokine receptors are the 7-transmembrane G-protein coupled receptors. Monocytes and macrophages express various chemokine receptors. Kupffer cells express CC-chemokine receptor 1 (CCR1), CCR2 and CCR5 that contribute to recruit inflammatory cells into inflammatory site in the liver(8-10). CX3CL1, also known as Fractalkine, is a membrane-bound type of chemokine. The soluble form of CX3CL1 is released after proteolysis by ADAM10 and ADAM17(11-13). CX3CL1 is involved in cell recruitment and cell survival through binding to CX3C-chemokine receptor 1 (CX3CR1) (14). The membrane-bound type of CX3CL1 binds to CX3CR1, which functions as an adhesion molecule independently of integrins(15). In addition, CX3CR1-expressing monocytes circulate in the steady state and differentiate into alternatively activated macrophages(16).

CCR2 promotes inflammation such as atherosclerosis, and lung, kidney and liver diseases by the trafficking of monocytes to inflammatory sites(8,17-19). In contrast, the role of CX3CR1 in inflammation is still controversial. CX3CR1-deficient mice had reduced inflammation and injury after kidney ischemia-reperfusion and in atherosclerosis(20-23). On the other hand, loss of CX3CR1 exaggerates LPS-induced neuronal damage, corneal neovascularization after alkali injury, and autoimmune uveitis and encephalomyelitis(24-27). CX3CL1 inhibits the production of nitric oxide, IL-6 and TNF-α in activated microglia, the resident macrophages in the central nervous system(28). Although increased CX3CL1 and CX3CR1 were observed in the livers of patients with chronic hepatitis C(29,30) and primary biliary cirrhosis(31), the precise role of the CX3CL1-CX3CR1 interaction in liver inflammation and fibrosis is unclear. Here we demonstrate that the disruption of CX3CR1 exacerbates liver inflammation and fibrosis by increased production of inflammatory and fibrogenic cytokines and reduced expression of IL-10 and arginase-1 in Kupffer cells. In addition, CX3CL1 treatment increases the expression of IL-10 and arginase-1 in Kupffer cells. These results suggest that the anti-inflammatory effects of CX3CR1 on Kupffer cells inhibit liver inflammation and fibrosis.

Material and Methods

Animal model of chronic liver inflammation

Specific pathogen-free wild-type (WT) C57BL/6J mice and C57BL/6 background $CX3CR1^{GFP/GFP}$ mice, in which the CX3CR1 allele is replaced with a GFP expressing cassette (Jackson Laboratories), were used(32). We used $CX3CR1^{GFP/GFP}$ mice as $CX3CR1^{-/-}$ mice(32). For the chronic liver inflammation model, mice were injected with CCl_4 diluted 1:3 in corn oil (Sigma) or vehicle (corn oil) intraperitoneally at a dose of 0.5 μl/g body weight twice a week for a total of 12 injections. Mice were sacrificed at 48 hours after the last injection. Serum levels of alanine aminotransferase (ALT) were measured using a commercial kit (Thermo Scientific). The mice received humane care according to National Institutes of Health recommendations outlined in *the Guide for the Care and Use of Laboratory Animals*. All animal experiments were approved by University of California, San Diego, Institutional Animal Care and Use committees.

Histological analysis

For immunohistochemical analysis, liver specimens were fixed in 10% buffered formalin and were incubated with monoclonal antibody against α-smooth muscle actin (α-SMA) (Sigma) using an M.O.M. kit (Vector Laboratories), rat anti mouse F4/80 (eBioscience) or rat anti mouse CD68 (AbD Serotec). For immunofluorescent staining, frozen sections were incubated with antibody to CX3CR1 (Novus Biologicals), F4/80, desmin (Neomarkers), pan-CK (Biolegend) or 4-hydroxy-nonenal (4-HNE) (Alpha Diagnostic) followed by imaging with fluorescent microscopy(8).

Isolation of Kupffer cells and HSCs

WT or CX3CR1-deficient mice were treated with intraperitoneal injection of CCl_4 or vehicle twice a week for 4 times. Then, liver cells were fractionated into 4 major cell populations (hepatocytes, Kupffer cells, endothelial cells and HSCs) as previously described(33). Briefly, mouse livers were digested by 2-step collagenase-pronase perfusion followed by 3-layer discontinuous density gradient centrifugation with 8.2% and 14.5% Nycodenz (Accurate Chemical and Scientific) to obtain hepatocyte fraction, Kupffer cell/endothelial cell fraction, and HSC fraction. Kupffer cell fraction and endothelial cell fraction were selected from Kupffer cell/endothelial cell fraction by magnetic cell sorting (MACS; Miltenyi Biotec) using anti-CD11b antibody and anti-liver sinusoidal endothelial cell antibody, respectively. HSCs were isolated by digestion with collagenase and pronase, followed by gradient centrifugation using 8.2% Nycodenz, and then $CD11b^+$ Kupffer cells were removed by MACS. More than 95% of the purity of isolated HSCs was confirmed by immunostaining with anti-desmin antibody.

Quantitative real-time polymerase chain reaction

Total RNA was prepared from cells or frozen liver tissues using TRIzol regent (Invitrogen), and cleaned by an RNeasy kit followed by DNase treatment (Qiagen). RNA was reverse transcribed using a high-capacity complementary DNA reverse-transcription kit (Applied Biosystems). Quantitative real-time PCR was performed using an ABI PRISM 7000 Sequence Detector (Applied Biosystems)(9). PCR primer sequences are listed in supplementary table 1. The expression of respective genes was normalized to 18S RNA as an internal control.

Flow cytometry

Liver mononuclear cells were prepared as previously described(10). Briefly, the liver was perfused and homogenated. The cells were resuspended in 36% Percoll and were centrifuged

at 700g for 10 minutes. After Fc receptor blockade, cells were stained with anti F4/80, CD11b and Ly6C (eBiociense). In some experiments, cells were isolated from $CX3CR1^{+/GFP}$ mice as CX3CR1-GFP reporter mice, in which both GFP and CX3CR1 are expressed under control of the endogenous CX3CR1 promoter, so that GFP expressing cells represent CX3CR1 expressing cells. Samples were analyzed on a BD FACSAria flow cytometer and analyzed using Flow-Jo software (Tree Star).

Treatment of primary Kupffer cells

Kupffer cells isolated from WT mice were cultured in RPMI 1640 medium (Invitrogen) containing 10% fetal bovine serum. After 24 hour incubation, medium were changed into RPMI 1640 medium containing 1% fetal bovine serum and then incubated with 100 ng/ml recombinant CX3CL1 (ProSpec) or vehicle (PBS) for additional 6 hours. In some experiments, Kupffer cells were pretreated with LY294002 (AKT inhibitor, 2μM, Sigma) or U0125 (ERK inhibitor, 20μM, Sigma) for 30 min before treating with CX3CL1(5,9).

Measurement of collagen-driven green fluorescent protein expression in HSCs

To measure collagen promoter activity, HSCs (1×10^5 cells/well) were isolated from collagen promoter-driven GFP transgenic mice (pCol9GFP-HS4,5 transgene)(34). HSCs were co-cultured with Kupffer cells (5×10^5 cells/well) for 48 hours in the presence or absence of 20 ng/ml soluble TGF-β receptor type II or 100ng/ml recombinant CX3CL1 (Prospec). Kupffer cells were isolated from WT or CX3CR1-deficient mice treated with or without CCl_4. The number of GFP-positive cells was determined by counting GFP-positive cells and total cells in ten randomly chosen high-power fields(5).

Cell migration assay

Cell migration assay was performed using a modified Boyden chamber as described previously(5). Briefly, WT Kupffer cells were placed onto the upper chamber (5×10^4 cells/well) in RPMI without serum and exposed to the vehicle or recombinant CX3CL1 (100 ng/ml) in the lower chamber. After 16 hours of incubation at 37°C, cells migrated to the lower side of the chamber were counted in 8 randomly chosen (× 100) fields.

Western blot

Preparation of whole cell protein extracts from frozen liver, electrophoresis and subsequent blotting were performed as previously described(35). We incubated blots with mouse antibody to α-SMA (Sigma), CYP2E1 (Millipore) and β-actin (Sigma), and then visualized by the enhanced chemiluminescence light method (Thermo Scientific).

Statistical Analysis

All data were expressed as mean ± standard error of the mean. Data between groups were analyzed by Student's *t*-tests. Differences between multiple groups were compared using one-way ANOVA (GraphPad Prism 4.02; GraphPad Software); *P*-values less than 0.05 were considered statistically significant.

Results

CX3CR1 is expressed on Kupffer cells in CCl_4-induced liver inflammation

To investigate whether CX3CR1 and its ligand CX3CL1 were involved in liver inflammation and fibrosis, hepatic mRNA expression of CX3CR1 and CX3CL1 was measured after 12 injections of CCl_4 in WT mice. Both CX3CR1 and CX3CL1 mRNA levels were significantly increased in the liver after CCl_4 treatment (Fig.1A). Next, we investigated the cellular source of CX3CR1 in the liver. CX3CR1 was expressed on F4/80

positive Kupffer cells/macrophages, but less CX3CR1 was detected on desmin positive HSCs (Fig.1B,C). CX3CR1 expression was not observed in hepatocytes, as determined by pan-CK immunostaining (Fig.1D). Subsequently, we measured mRNA expression of CX3CR1 and CX3CL1 on hepatocytes, Kupffer cells/macrophages and HSCs isolated from vehicle- or CCl_4-treated mice. CX3CR1 mRNA was preferentially expressed in Kupffer cells/macrophages, and further increased after CCl_4 treatment (Fig.1E). FACS analysis determined ~15% of F4/80 positive cells expressed CX3CR1, which was further increased to ~45% after CCl_4 treatment. Ly6C is mainly expressed on bone marrow-derived infiltrated macrophages(10,36), and CX3CR1 is largely expressed on Ly6C-negative monocytes in other organs, such as intestines(16,37). Similarly, CX3CR1 was more highly expressed on Ly6C-negative macrophages in the liver (Fig. 1F).

Increased liver inflammation in CX3CR1-deficient mice after chronic treatment with CCl_4

To investigate the role of CX3CR1 in liver inflammation, WT and CX3CR1-deficient mice were treated with 12 injections of CCl_4. Hepatic mRNA expression of inflammatory cytokine was measured by quantitative real-time PCR. After treatment of CCl_4, hepatic inflammatory gene expression including TNF-α, MCP-1, MIP-1α, MIP-1β, and RANTES was significantly increased in CX3CR1-deficient mice compared with WT mice (Fig.2A). Inflammatory cell infiltration was enhanced in CX3CR1-deficient mice treated with CCl_4 as determined by H-E staining (Fig.2B). Serum ALT levels were markedly elevated in CX3CR1-deficient mice compared with WT mice after CCl_4 injections (Fig.2C). Because CYP2E1-mediated CCl_4 metabolism plays an essential role in CCl_4-induced liver damage(38), we examined CYP2E1 expression and generation of oxidative stress. We did not observe any differences in CYP2E1 levels and oxidative stress (Sup.Fig.1A,B) between WT and CX3CR1-deficient mice after CCl_4-treatment. These results demonstrate that loss of CX3CR1 exacerbates liver inflammation and injury induced by CCl_4 treatment.

Macrophage infiltration is increased in CX3CR1-deficient mice after CCl_4 treatment

To further investigate liver inflammation in CX3CR1-deficient mice, macrophage infiltration and activation were assessed. Following CCl_4 treatment, the expression of F4/80, and CD68, an activation marker for macrophages, was significantly increased in CX3CR1-deficient livers compared with WT livers as determined by immunohistochemistry and quantitative real time PCR(Fig.3A-E). FACS analysis demonstrated that the number of $F4/80^+$ Kupffer cells was decreased in CX3CR1-deficient mice compared to WT mice treated with vehicle (WT vs $CX3CR1^{-/-}$ = 25.94 % vs 16.98%) (Fig.3F). CCl_4 treatment increased the $CD11b^+F4/80^+$ population in WT mice (Vehicle vs CCl_4 = 6.04 % vs 8.57 %). $CD11b^+F4/80^+$ cells were more increased in CX3CR1-deficient livers after CCl_4 treatment (Vehicle vs CCl_4 = 2.58 % vs 12.4 %) (Fig.3F).

Enhanced inflammatory features in CX3CR1-deficient Kupffer cells

To characterize CX3CR1-deficient macrophages in the liver, liver Kupffer cells/ macrophages were isolated from the control and fibrotic livers of both WT and CX3CR1-deficient mice. Compared with macrophages from WT livers, TNF-α and TGF-β1 mRNA levels were markedly increased in macrophages of CCl_4-treated CX3CR1-deficient mice (Fig.4A). Of note, mRNA expression of anti-inflammatory markers, IL-10 and arginase-1 was significantly reduced in macrophages of CCl_4-treated CX3CR1-deficient mice compared to those of CCl_4-treated WT mice or control CX3CR1-deficient mice (Fig.4B). These results demonstrate that pro-inflammatory properties are augmented and anti-inflammatory properties are diminished in CX3CR1-deficient macrophages.

CX3CL1 induces anti-inflammatory features and migration of Kupffer cells

The enhanced inflammatory features of CX3CR1-deficient Kupffer cells/macrophages prompted us to study the interaction of CX3CL1-CX3CR1 in Kupffer cells. WT Kupffer cells were treated with CX3CL1 for 6 hours followed by measuring the expression of anti-inflammatory markers. mRNA levels of IL-10 and arginase-1 were significantly increased in CX3CL1-treated WT, but not CX3CR1-deficient, Kupffer cells (Fig. 5A). Since CX3CL1-CX3CR1 interaction induces AKT and ERK activation(39), we tested the requirement of AKT and ERK in CX3CL1-CX3CR1 signaling. Inhibition of AKT or ERK blocked IL-10 and arginase-1 expression in CX3CL1-treated Kupffer cells (Supp.Fig.2). These results demonstrate that CX3CL1 induces anti-inflammatory properties through CX3CR1, AKT and ERK. Moreover, CX3CL1 increased migration of CD11b+ Kupffer cells/macrophages (Fig. 5B). As shown in Figure 1, CX3CR1 expression in HSCs is very low. To exclude the possibility that low levels of CX3CR1 contribute to HSC activation, we examined HSC activation treated with CX3CL1 by assessing collagen α1(I) promoter activity using HSCs isolated from collagen promoter-driven GFP transgenic (Coll-GFP) mice (Fig.5C). CX3CL1 treatment did not have any effect on the enhancement of GFP expression and collagen α1(I) mRNA expression in HSCs (Fig.5C-E). These results suggest that CX3CL1-CX3CR1 interaction induces Kupffer cell migration and anti-inflammatory features, but does not induce HSC activation.

CX3CR1-deficient Kupffer cells enhance HSC activation *via* TGF-β

Inflammatory and fibrogenic cytokine production was augmented in CX3CR1-deficient Kupffer cells (Fig.4). To investigate whether Kupffer cells of CX3CR1-deficient mice enhance HSC activation, HSCs of Coll-GFP mice were co-cultured with Kupffer cells from control and fibrotic livers of either WT or CX3CR1-deficient mice. HSCs expressed higher GFP fluorescence in co-cultures with Kupffer cells of CCl_4-treated CX3CR1-deficient mice compared to those of other mouse groups (Fig.6A,B). Next, we treated co-culturing of HSCs and Kupffer cells with the TGF-β receptor inhibitor, the soluble form of type II TGF-β receptor. GFP expression of HSCs was significantly suppressed by treating with soluble type II TGF-β receptor (Fig.6A,B), suggesting that enhanced HSC activation by CX3CR1-deficient Kupffer cells requires TGF-β. Moreover, we examined if exogenous CX3CL1 treatment suppresses HSC activation co-cultured with Kupffer cells. CX3CL1 treatment inhibits Coll-GFP HSCs co-cultured with Kupffer cells from CCl_4-treated WT, but not CX3CR1-deficient, mice (Fig.6). These results suggest that CX3CL1 suppresses HSC activation through CX3CR1 on Kupffer cells. Further therapeutic potential of CX3CL1 was investigated in LPS-treated Kupffer cells. CX3CL1 treatment suppressed TNF-α and TGF-β induction in Kupffer cells in response to LPS (Supp.Fig.3). Thus, the CX3CL1-CX3CR1 interaction inhibits the inflammatory property but induces the anti-inflammatory property in Kupffer cells.

Liver fibrosis is exacerbated in CX3CR1-deficient mice after CCl_4 treatment

Finally, we examined liver fibrosis in CX3CR1-deficient mice. Fibrogenic markers including collagen α1(I), TIMP-1 and TGF-β1 mRNA levels were significantly increased in CX3CR1-deficient mice compared with WT mice after CCl_4 treatment (Fig.7A). Fibrillar collagen deposition was markedly increased in CX3CR1-deficient mice, as assessed by Sirius red staining and its quantification (Fig.7B,C). Hepatic α-SMA expression, a marker for HSC activation, was enhanced in CX3CR1-deficient mice compared to that in WT mice, as assessed by immunohistochemistry and immunoblotting (Fig.7D,E). These results demonstrate that enhanced activation of Kupffer cells increases HSC activation and fibrosis in CX3CR1-deficient mice after CCl_4 treatment.

Discussion

A key function of chemokine-chemokine receptor interaction is chemoattractant activity. Recent studies have shown that their role is not only in cell migration, but also in inflammation, fibrogenesis and cell survival(6,23). The present study demonstrates that CX3CR1 deficiency exacerbates liver inflammation and injury. Kupffer cells from CX3CR1-deficient mice lose their anti-inflammatory features including IL-10 and arginase-1 expression, and enhance the expression of inflammatory cytokines and chemokines. Increased fibrogenic cytokines including TGF-β induce a strong activation of HSCs leading to more liver fibrosis. Recombinant soluble CX3CL1 increases the expression of IL-10 and arginase-1 in Kupffer cells, which inhibit fibrogenic responses(40-43). These findings suggest that the CX3CL1-CX3CR1 interaction induces “alternative” activated macrophages that have anti-inflammatory properties, preventing excessive liver inflammation and fibrosis.

Chemokines are generally believed to act by recruiting immune cells that induce inflammation(7). Our previous studies have shown that CCR1, CCR2 and CCR5 signaling promote liver inflammation and fibrosis(8,9). Kupffer cells express CCR1, CCR2 and CCR5. The activation of these chemokine receptors results in migration of macrophage into the injured site, which leads to inflammation and HSC activation, resulting in fibrosis(3). These “classical” inflammatory macrophages preferentially express iNOS, IL-12 and TNF-α and also express Ly6C. Interestingly, the functions of CX3CL1-CX3CR1 axis are organ and disease specific. In atherosclerosis, inactivation of CX3CL1 or CX3CR1 reduces the severity(21,23). Therefore, CX3CR1 antagonists are being developed for the therapy of atherosclerosis(44). On the other hand, the CX3CL1-CX3CR1 interaction exerts anti-inflammatory effects in microglia and neurons to protect the central nervous system from injury(28), which corroborates our study that CX3CR1 negatively regulates liver inflammation and fibrosis. Kupffer cells/macrophages express CX3CR1, which is further increased after CCl_4 treatment (Fig.1F). Hepatic NK cells and T cells also express CX3CR1(45), but the expression was not increased after CCl_4 treatment (Sup.Fig.4). Thus, we suggest that CX3CR1 on Kupffer cells/macrophages to induce “alternative” activated macrophages is critical in modulating liver inflammation.

Previous studies demonstrated that disruption of CX3CR1 reduces $Ly6C^{low}$ monocytes due to apoptosis(14). Overexpressed hBcl-2 in CX3CR1-deficient mice restores the reduction of $Ly6C^{low}$ monocytes to normal(14). Furthermore, recombinant CX3CL1 treatment increases the survival of monocytes from serum deprivation and oxysterol-induced death(14). These findings suggest that CX3CL1-CX3CR1 interaction prevents monocyte apoptosis, which could explain the decreased number of hepatic macrophages in control CX3CR1-deficient mice (Fig.3F). On the other hand, the number of monocytes/macrophages is increased in the livers of CX3CR1-deficinet mice compared to those of WT mice after CCl_4 treatment. Increased CC-chemokines in CCl_4-treated CX3CR1-deficient mice (Fig.2A) could recruit inflammatory cells through CCR1, CCR2 and CCR5, independent of CX3CR1(8-10).

CX3CL1 is an exclusive ligand for CX3CR1 and is produced as a membrane bound form(13,15). Therefore, CX3CL1-CX3CR1 interaction not only induces cell migration, but also acts as an adhesion molecule for the capture and firm adhesion of CX3CL1- and/or CX3CR1-expressing cells during cell recruitment and trafficking(15). As shown in Figure 1, HSCs express much higher levels of CX3CL1 than Kupffer cells (Fig.1E). CX3CR1 on Kupffer cells and the membrane bound type of CX3CL1 on HSCs might interact directly and be important for Kupffer cell-HSC interaction, which is important for HSC activation. A previous study showed that HSCs suppress immune cell activation(46). Our data demonstrate that HSC activation is increased in co-cultures with CX3CR1-deficient Kupffer

cells, and is inhibited in co-cultures with WT Kupffer cells treated with CX3CL1 (Fig. 6). CX3CL1 treatment also suppressed LPS-induced TNF-α and TGF-β production in Kupffer cells, which is consistent with a previous study using microglia(28). Thus, Kupffer cell-HSC interaction activates HSCs and produce inflammatory chemokines MCP-1 and RANTES, but also prevents excessive activation of Kupffer cells/macrophages through the binding of HSC-derived CX3CL1 to the CX3CR1 on Kupffer cells, inhibiting HSC activation.

Clinical observations have demonstrated a correlation between the hepatic mRNA levels of CX3CR1 and the severity of histological fibrosis score in patients with chronic hepatitis C(29,30). CX3CL1 and CX3CR1 levels are also increased in the livers of patients with primary billiary cirrhosis, primary sclerosing cholangitis and extrahepatic biliary obstruction(31). In these patients, CX3CR1 is not only expressed on leukocytes, but also on pathological biliary epithelial cells. Moreover, patients with chronic hepatitis C with the CX3CR1 V249I polymorphism have more severe liver fibrosis and hepatic TIMP-1 mRNA levels(29). Leukocytes that express the CX3CR1 V249I variant have reduced binding activity with CX3CL1(47), which corroborates our result that CX3CR1 signaling negatively regulates liver inflammation. We suggest that increased CX3CR1 expression in severe liver fibrosis in humans and mice might inhibit liver fibrosis(29-31). Thus, modulation of CX3CL1-CX3CR1 interaction may become a useful therapeutic target for chronic liver inflammation and fibrosis.

Supplementary Material

Refer to Web version on PubMed Central for supplementary material.

Acknowledgments

Grant support: This study is supported by a Liver Scholar Award from the American Association for the Study of Liver Diseases/ American Liver Foundation, a research grant from ABMRF, and a pilot project from the Southern California Research Center for ALPD and Cirrhosis (P50 AA11999) funded by NIAAA (to ES) and NIH grant 5R01GM041804 (DAB).

References

1. Crispe IN. The liver as a lymphoid organ. Annu Rev Immunol. 2009; 27:147–163. [PubMed: 19302037]
2. Tacke F, Luedde T, Trautwein C. Inflammatory pathways in liver homeostasis and liver injury. Clin Rev Allergy Immunol. 2009; 36:4–12. [PubMed: 18600481]
3. Bataller R, Brenner DA. Liver fibrosis. J Clin Invest. 2005; 115:209–218. [PubMed: 15690074]
4. Friedman SL. Mechanisms of hepatic fibrogenesis. Gastroenterology. 2008; 134:1655–1669. [PubMed: 18471545]
5. Seki E, De Minicis S, Osterreicher CH, Kluwe J, Osawa Y, Brenner DA, Schwabe RF. TLR4 enhances TGF-beta signaling and hepatic fibrosis. Nat Med. 2007; 13:1324–1332. [PubMed: 17952090]
6. Bachmann MF, Kopf M, Marsland BJ. Chemokines: more than just road signs. Nat Rev Immunol. 2006; 6:159–164. [PubMed: 16491140]
7. Jin T, Xu X, Hereld D. Chemotaxis, chemokine receptors and human disease. Cytokine. 2008; 44:1–8. [PubMed: 18722135]
8. Seki E, de Minicis S, Inokuchi S, Taura K, Miyai K, van Rooijen N, Schwabe RF, et al. CCR2 promotes hepatic fibrosis in mice. Hepatology. 2009; 50:185–197. [PubMed: 19441102]
9. Seki E, De Minicis S, Gwak GY, Kluwe J, Inokuchi S, Bursill CA, Llovet JM, et al. CCR1 and CCR5 promote hepatic fibrosis in mice. J Clin Invest. 2009; 119:1858–1870. [PubMed: 19603542]

10. Karlmark KR, Weiskirchen R, Zimmermann HW, Gassler N, Ginhoux F, Weber C, Merad M, et al. Hepatic recruitment of the inflammatory Gr1+ monocyte subset upon liver injury promotes hepatic fibrosis. Hepatology. 2009; 50:261–274. [PubMed: 19554540]
11. Garton KJ, Gough PJ, Blobel CP, Murphy G, Greaves DR, Dempsey PJ, Raines EW. Tumor necrosis factor-alpha-converting enzyme (ADAM17) mediates the cleavage and shedding of fractalkine (CX3CL1). J Biol Chem. 2001; 276:37993–38001. [PubMed: 11495925]
12. Hundhausen C, Misztela D, Berkhout TA, Broadway N, Saftig P, Reiss K, Hartmann D, et al. The disintegrin-like metalloproteinase ADAM10 is involved in constitutive cleavage of CX3CL1 (fractalkine) and regulates CX3CL1-mediated cell-cell adhesion. Blood. 2003; 102:1186–1195. [PubMed: 12714508]
13. Bourd-Boittin K, Basset L, Bonnier D, L'Helgoualc'h A, Samson M, Theret N. CX3CL1/fractalkine shedding by human hepatic stellate cells: contribution to chronic inflammation in the liver. J Cell Mol Med. 2009; 13:1526–1535. [PubMed: 19432809]
14. Landsman L, Bar-On L, Zernecke A, Kim KW, Krauthgamer R, Shagdarsuren E, Lira SA, et al. CX3CR1 is required for monocyte homeostasis and atherogenesis by promoting cell survival. Blood. 2009; 113:963–972. [PubMed: 18971423]
15. Fong AM, Robinson LA, Steeber DA, Tedder TF, Yoshie O, Imai T, Patel DD. Fractalkine and CX3CR1 mediate a novel mechanism of leukocyte capture, firm adhesion, and activation under physiologic flow. J Exp Med. 1998; 188:1413–1419. [PubMed: 9782118]
16. Auffray C, Fogg D, Garfa M, Elain G, Join-Lambert O, Kayal S, Sarnacki S, et al. Monitoring of blood vessels and tissues by a population of monocytes with patrolling behavior. Science. 2007; 317:666–670. [PubMed: 17673663]
17. Boring L, Gosling J, Cleary M, Charo IF. Decreased lesion formation in CCR2-/- mice reveals a role for chemokines in the initiation of atherosclerosis. Nature. 1998; 394:894–897. [PubMed: 9732872]
18. Boring L, Gosling J, Chensue SW, Kunkel SL, Farese RV Jr, Broxmeyer HE, Charo IF. Impaired monocyte migration and reduced type 1 (Th1) cytokine responses in C-C chemokine receptor 2 knockout mice. J Clin Invest. 1997; 100:2552–2561. [PubMed: 9366570]
19. Kitagawa K, Wada T, Furuichi K, Hashimoto H, Ishiwata Y, Asano M, Takeya M, et al. Blockade of CCR2 ameliorates progressive fibrosis in kidney. Am J Pathol. 2004; 165:237–246. [PubMed: 15215179]
20. Li L, Huang L, Sung SS, Vergis AL, Rosin DL, Rose CE Jr, Lobo PI, et al. The chemokine receptors CCR2 and CX3CR1 mediate monocyte/macrophage trafficking in kidney ischemia-reperfusion injury. Kidney Int. 2008; 74:1526–1537. [PubMed: 18843253]
21. Lesnik P, Haskell CA, Charo IF. Decreased atherosclerosis in CX3CR1-/- mice reveals a role for fractalkine in atherogenesis. J Clin Invest. 2003; 111:333–340. [PubMed: 12569158]
22. Furuichi K, Gao JL, Murphy PM. Chemokine receptor CX3CR1 regulates renal interstitial fibrosis after ischemia-reperfusion injury. Am J Pathol. 2006; 169:372–387. [PubMed: 16877340]
23. Tacke F, Alvarez D, Kaplan TJ, Jakubzick C, Spanbroek R, Llodra J, Garin A, et al. Monocyte subsets differentially employ CCR2, CCR5, and CX3CR1 to accumulate within atherosclerotic plaques. J Clin Invest. 2007; 117:185–194. [PubMed: 17200718]
24. Cardona AE, Pioro EP, Sasse ME, Kostenko V, Cardona SM, Dijkstra IM, Huang D, et al. Control of microglial neurotoxicity by the fractalkine receptor. Nat Neurosci. 2006; 9:917–924. [PubMed: 16732273]
25. Lu P, Li L, Kuno K, Wu Y, Baba T, Li YY, Zhang X, et al. Protective roles of the fractalkine/CX3CL1-CX3CR1 interactions in alkali-induced corneal neovascularization through enhanced antiangiogenic factor expression. J Immunol. 2008; 180:4283–4291. [PubMed: 18322241]
26. Dagkalis A, Wallace C, Hing B, Liversidge J, Crane IJ. CX3CR1-deficiency is associated with increased severity of disease in experimental autoimmune uveitis. Immunology. 2009; 128:25–33. [PubMed: 19689733]
27. Sunnemark D, Eltayeb S, Nilsson M, Wallstrom E, Lassmann H, Olsson T, Berg AL, et al. CX3CL1 (fractalkine) and CX3CR1 expression in myelin oligodendrocyte glycoprotein-induced experimental autoimmune encephalomyelitis: kinetics and cellular origin. J Neuroinflammation. 2005; 2:17. [PubMed: 16053521]

28. Zujovic V, Benavides J, Vige X, Carter C, Taupin V. Fractalkine modulates TNF-alpha secretion and neurotoxicity induced by microglial activation. Glia. 2000; 29:305–315. [PubMed: 10652441]
29. Wasmuth HE, Zaldivar MM, Berres ML, Werth A, Scholten D, Hillebrandt S, Tacke F, et al. The fractalkine receptor CX3CR1 is involved in liver fibrosis due to chronic hepatitis C infection. J Hepatol. 2008; 48:208–215. [PubMed: 18078680]
30. Efsen E, Grappone C, DeFranco RM, Milani S, Romanelli RG, Bonacchi A, Caligiuri A, et al. Up-regulated expression of fractalkine and its receptor CX3CR1 during liver injury in humans. J Hepatol. 2002; 37:39–47. [PubMed: 12076860]
31. Isse K, Harada K, Zen Y, Kamihira T, Shimoda S, Harada M, Nakanuma Y. Fractalkine and CX3CR1 are involved in the recruitment of intraepithelial lymphocytes of intrahepatic bile ducts. Hepatology. 2005; 41:506–516. [PubMed: 15726664]
32. Jung S, Aliberti J, Graemmel P, Sunshine MJ, Kreutzberg GW, Sher A, Littman DR. Analysis of fractalkine receptor CX(3)CR1 function by targeted deletion and green fluorescent protein reporter gene insertion. Mol Cell Biol. 2000; 20:4106–4114. [PubMed: 10805752]
33. Taura K, De Minicis S, Seki E, Hatano E, Iwaisako K, Osterreicher CH, Kodama Y, et al. Hepatic stellate cells secrete angiopoietin 1 that induces angiogenesis in liver fibrosis. Gastroenterology. 2008; 135:1729–1738. [PubMed: 18823985]
34. Magness ST, Bataller R, Yang L, Brenner DA. A dual reporter gene transgenic mouse demonstrates heterogeneity in hepatic fibrogenic cell populations. Hepatology. 2004; 40:1151–1159. [PubMed: 15389867]
35. Aoyama T, Ikejima K, Kon K, Okumura K, Arai K, Watanabe S. Pioglitazone promotes survival and prevents hepatic regeneration failure after partial hepatectomy in obese and diabetic KK-A(y) mice. Hepatology. 2009; 49:1636–1644. [PubMed: 19205029]
36. Lin SL, Castano AP, Nowlin BT, Lupher ML Jr, Duffield JS. Bone marrow Ly6Chigh monocytes are selectively recruited to injured kidney and differentiate into functionally distinct populations. J Immunol. 2009; 183:6733–6743. [PubMed: 19864592]
37. Geissmann F, Jung S, Littman DR. Blood monocytes consist of two principal subsets with distinct migratory properties. Immunity. 2003; 19:71–82. [PubMed: 12871640]
38. Basu S. Carbon tetrachloride-induced lipid peroxidation: eicosanoid formation and their regulation by antioxidant nutrients. Toxicology. 2003; 189:113–127. [PubMed: 12821287]
39. Davis CN, Harrison JK. Proline 326 in the C terminus of murine CX3CR1 prevents G-protein and phosphatidylinositol 3-kinase-dependent stimulation of Akt and extracellular signal-regulated kinase in Chinese hamster ovary cells. J Pharmacol Exp Ther. 2006; 316:356–363. [PubMed: 16166268]
40. Pesce JT, Ramalingam TR, Mentink-Kane MM, Wilson MS, El Kasmi KC, Smith AM, Thompson RW, et al. Arginase-1-expressing macrophages suppress Th2 cytokine-driven inflammation and fibrosis. PLoS Pathog. 2009; 5:e1000371. [PubMed: 19360123]
41. Louis H, Van Laethem JL, Wu W, Quertinmont E, Degraef C, Van den Berg K, Demols A, et al. Interleukin-10 controls neutrophilic infiltration, hepatocyte proliferation, and liver fibrosis induced by carbon tetrachloride in mice. Hepatology. 1998; 28:1607–1615. [PubMed: 9828225]
42. Huang YH, Shi MN, Zheng WD, Zhang LJ, Chen ZX, Wang XZ. Therapeutic effect of interleukin-10 on CCl4-induced hepatic fibrosis in rats. World J Gastroenterol. 2006; 12:1386–1391. [PubMed: 16552806]
43. Nelson DR, Lauwers GY, Lau JY, Davis GL. Interleukin 10 treatment reduces fibrosis in patients with chronic hepatitis C: a pilot trial of interferon nonresponders. Gastroenterology. 2000; 118:655–660. [PubMed: 10734016]
44. Dorgham K, Ghadiri A, Hermand P, Rodero M, Poupel L, Iga M, Hartley O, et al. An engineered CX3CR1 antagonist endowed with anti-inflammatory activity. J Leukoc Biol. 2009; 86:903–911. [PubMed: 19571253]
45. Heydtmann M, Adams DH. Chemokines in the immunopathogenesis of hepatitis C infection. Hepatology. 2009; 49:676–688. [PubMed: 19177577]
46. Yang HR, Chou HS, Gu X, Wang L, Brown KE, Fung JJ, Lu L, et al. Mechanistic insights into immunomodulation by hepatic stellate cells in mice: a critical role of interferon-gamma signaling. Hepatology. 2009; 50:1981–1991. [PubMed: 19821484]

47. Moatti D, Faure S, Fumeron F, Amara Mel W, Seknadji P, McDermott DH, Debre P, et al. Polymorphism in the fractalkine receptor CX3CR1 as a genetic risk factor for coronary artery disease. Blood. 2001; 97:1925–1928. [PubMed: 11264153]

Abbreviations

ADAM	adisintegrin and metalloprotease
ALT	alanine aminotransferase
CX3CL	CX3C-chemokine ligand
CCl_4	carbon tetrachloride
CCR	CC-chemokine receptor
CX3CR	CX3C-chemokine receptor
ECM	extracellular matrix
GFP	green fluorescent protein
FBS	fetal bovine serum
HSC	hepatic stellate cell
IL	interleukin
KO	knockout
LPS	lipopolysaccharide
MCP	monocyte chemoattractant protein
MIP	macrophage inflammatory proteins
MMP	matrix metalloproteinase
PBS	phosphate buffered saline
PCR	polymerase chain reaction
RANTES	regulated on activation normal T cell expressed and secreted
SMA	smooth muscle actin
TGF	transforming growth factor
TIMP	tissue inhibitor of metalloproteinase
TNF	tumor necrosis factor
WT	wild-type

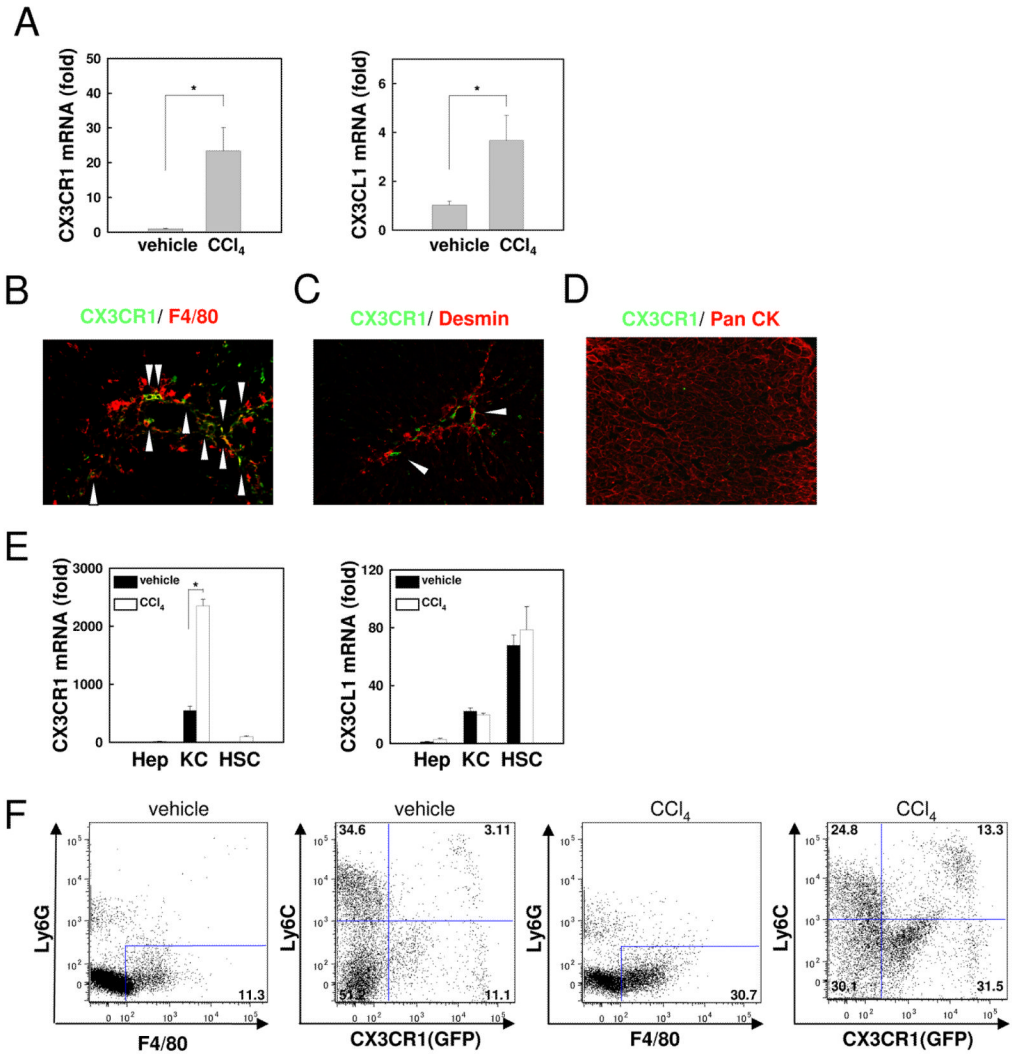

Fig 1. Kupffer cells/macrophages express CX3CR1 in the liver

Livers were analyzed from WT mice after 12 injections of CCl_4 or vehicle (n=5). (A) Hepatic mRNA expression of CX3CR1 and CX3CL1 was measured by quantitative real time PCR. (B-D) CX3CR1 expression (in green) was detected by co-staining with (B) F4/80 (in red), (C) desmin (in red), and (D) pan-cytokeratin (in red) by fluorescence microscopy. Arrows indicate CX3CR1-positive and (B) F4/80 positive or (C) desmin positive cells. (E) mRNA levels of CX3CR1 and CX3CL1 in hepatocytes, Kupffer cells and HSCs isolated from vehicle- or CCl_4-treated WT mice were detected by quantitative real time PCR (n=3). (F) Liver mononuclear cells isolated from control or CCl_4-treated $CX3CR1^{+/GFP}$ mice, were stained with anti-F4/80, Ly6G, and Ly6C antibody followed by FACS analysis. F4/80 positive Ly6G negative cells were analyzed for Ly6C and GFP, as a measure of endogenous CX3CR1 expression. Representative FACS analysis is shown (n=3). * $P<0.05$.

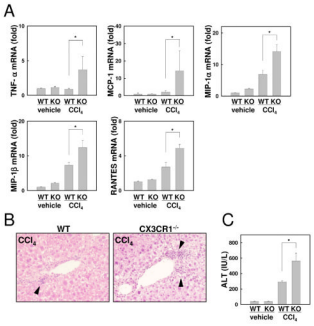

Fig 2. Loss of CX3CR1 exacerbated liver inflammation after chronic treatment with CCl_4

Chronic hepatitis was induced by intraperitoneal injection with CCl_4 or vehicle twice a week for a total of 12 injections in WT (n=5) or CX3CR1$^{-/-}$ (KO) mice (n=5). (A) Hepatic mRNA expressions of TNF-α, MCP-1, MIP-1α, MIP-1β, and RANTES were measured by quantitative real time PCR. (B) Liver histology of CCl_4-treated WT and CX3CR1$^{-/-}$ mice is assessed by H-E staining (original magnification: ×200). Arrows indicate inflammatory cell infiltration. (C) Serum ALT levels were measured. *P<0.05.

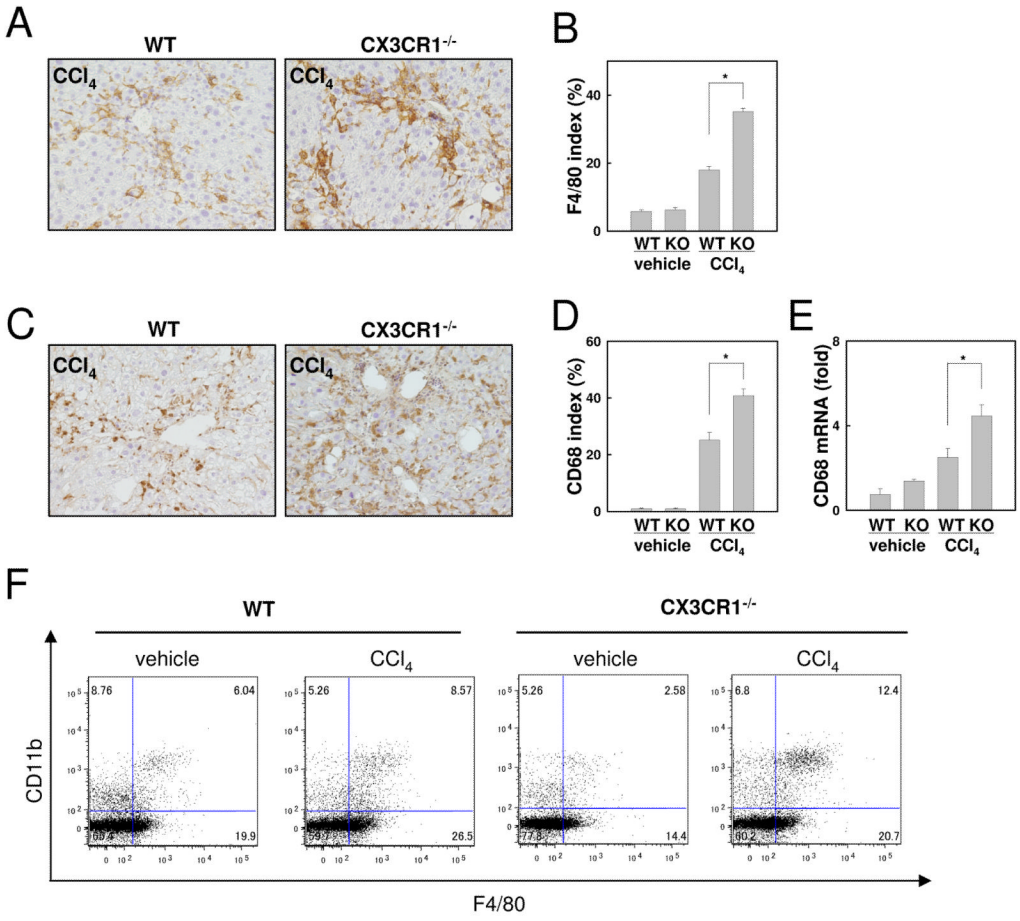

Fig 3. Increased macrophage infiltration in CCl_4-treated CX3CR1-deficient mice

WT (n=5) or CX3CR1$^{-/-}$ (KO) mice (n=5) were intraperitoneally injected with CCl_4 or vehicle 12 times. (A-D) Immmunohistochemistry for F4/80 (A) and CD68 (C), and (B, D) their quantification are shown (original magnification: ×200). (E) Hepatic mRNA expression of CD68 was measured by quantitative real time PCR. (F) Representative FACS analysis for F4/80 and CD11b expression in WT or CX3CR1$^{-/-}$ livers are shown (n=3). *P<0.05.

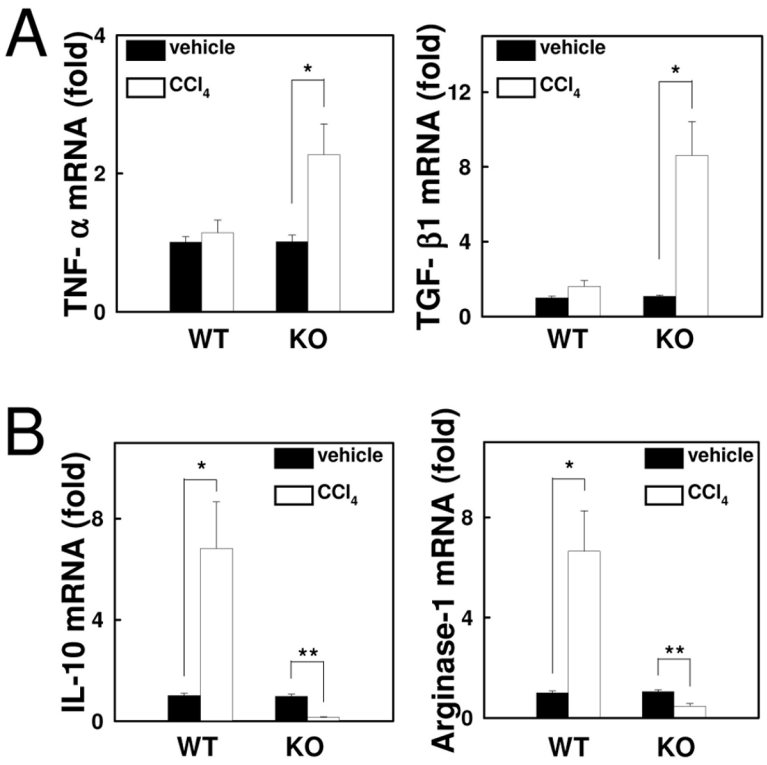

Fig 4. CX3CR1-deficient Kupffer cells have augmented inflammatory properties

Kupffer cells were isolated from WT or CX3CR1$^{-/-}$ (KO) mice treated with CCl_4 or vehicle for 4 times (n=3). (A, B) mRNA levels of (A) TNF-α, TGF-β1, (B) IL-10 and arginase-1 were measured by quantitative real time PCR. *P<0.05, **P<0.01.

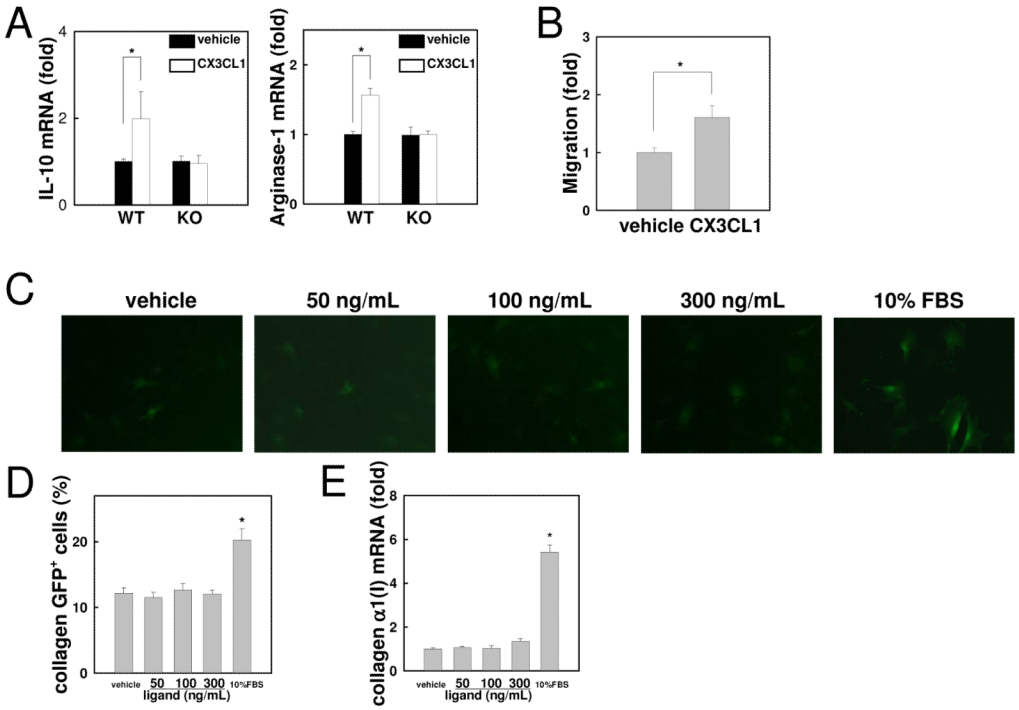

Fig 5. CX3CL1 induces alternative activation of Kupffer cells by expressing IL-10 and arginase-1 through CX3CR1

Kupffer cells isolated from WT and CX3CR1-deficient mice were incubated with 100 ng/ml CX3CL1 or vehicle (PBS). (A) mRNA levels of IL-10 and arginase-1 were measured by quantitative real time PCR. (B) Serum-free media containing recombinant CX3CL1 (100 ng/mL) was placed in the lower chamber and Kupffer cells of WT mice were placed in the upper chamber. Migration of Kupffer cells into the lower chamber was counted 16 hours after stimulation. (C, D) HSCs of collagen promoter driven GFP transgenic mice were incubated with 50, 100 or 300 ng/ml recombinant CX3CL1 or vehicle (PBS) for 48 hours. (C) Representative photomicrographs of HSCs and (D) their quantification are shown (original magnification: ×200). (E) Collagen α1(I) mRNA are shown. Similar results were obtained in three independent experiments. *P<0.05.

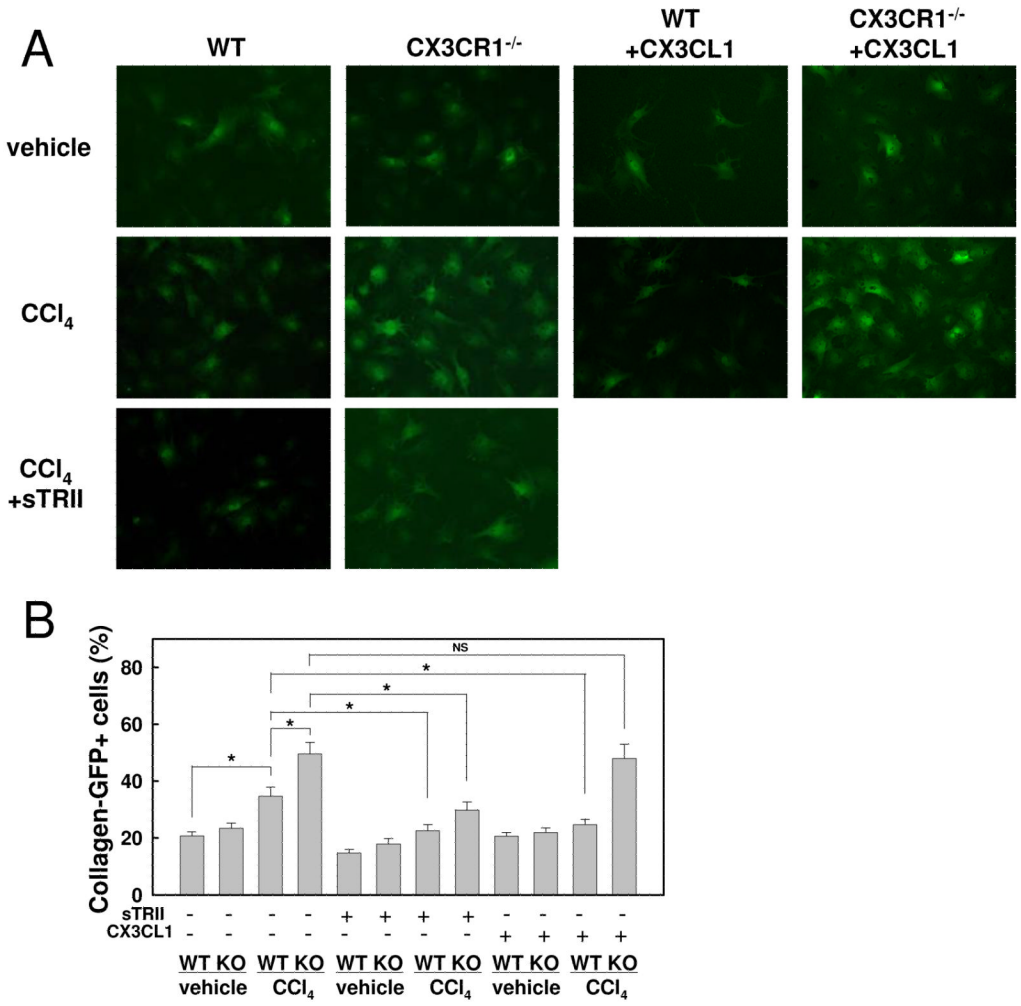

Fig 6. CX3CR1-deficient Kupffer cells enhanced and CX3CL1 treatment inhibited HSC activation

HSCs isolated from collagen promoter-driven GFP transgenic mice were co-cultured with WT or CX3CR1$^{-/-}$ Kupffer cells for 48 hours in the presence or absence of 20 ng/ml soluble TGF-β receptor type II, or 100ng/ml recombinant CX3CL1. (A) Representative photomicrographs of GFP positive HSCs and (B) their quantification are shown (original magnification: ×200). A representative result is shown. Similar results were obtained in three independent experiments. *P<0.05.

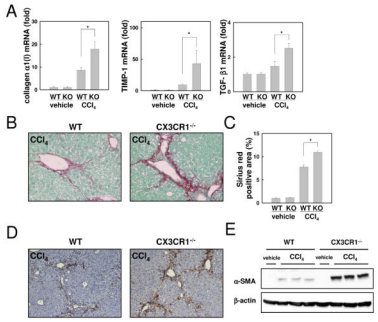

Fig 7. Increased Liver fibrosis in CX3CR1-deficient mice after CCl_4 treatment

WT (n=5) or CX3CR1$^{-/-}$ (KO) mice (n=5) were treated with CCl_4 or vehicle for 12 times. (A) Hepatic mRNA expressions of collagen α1(I), TIMP-1 and TGF-β1 mRNA were measured by quantitative real time PCR. (B) Fibrillar collagen deposition was evaluated by Sirius red staining (original magnification: ×200) and (C) its quantification. (D, E) Expression α-SMA in the liver was detected by immunohistochemistry (D) and western blotting (E). (original magnification: ×100). *P<0.05.